Electron-phonon interactions and high-temperature thermodynamics of vanadium and its alloys

O. Delaire, M. Kresch, J. A. Muñoz, M. S. Lucas, J. Y. Y. Lin, and B. Fultz
W. M. Keck Laboratory, mail 138-78, California Institute of Technology, Pasadena, California 91125, USA
(Received 1 May 2008; published 25 June 2008)

Inelastic neutron scattering was used to measure the phonon densities of states (DOSs) for pure V and solid solutions of V with 6 to 7at% of Co, Nb, and Pt, at temperatures from 10 K to 1323 K. Ancillary measurements of heat capacity and thermal expansion are reported on V and V-7at%Co and used to help identify the different sources of entropy. Pure V exhibits an anomalous anharmonic stiffening of phonons with increasing temperature. This anharmonicity is suppressed by Co and Pt, but not by isoelectronic Nb solutes. The changes in phonon frequency with alloying and with temperature both correlate to the decrease in electron density of states (DOS) at the Fermi level as calculated using density functional theory. The effects of both temperature and alloying can be understood in terms of an adiabatic electron-phonon interaction (EPI), which broadens sharp features in the electron DOS. These results show that the adiabatic EPI can influence the phonon thermodynamics at temperatures exceeding 1000 K, and that thermal trends of phonons may help assess the strength of the EPI.

DOI: 10.1103/PhysRevB.77.214112 PACS number(s): 63.20.K−, 61.05.F−, 71.20.Be, 74.25.Bt

I. INTRODUCTION

The body-centered cubic (bcc) transition metals V and Nb are among the elements with the strongest electron-phonon coupling,[1] and have attracted recent interest for their superconductive, electronic, and elastic properties at high pressures.[2–5] Effects of the electron-phonon interaction (EPI) are known for specific phonons in Nb and Nb-Mo alloys, where anomalous softening of the dispersion curves has been reported.[6–8] Naïvely, however, we expect the overall thermodynamic effects of the EPI to be much weaker than for the phonon-phonon interaction (PPI) by the ratio of the Debye temperature to the Fermi temperature. A deeper argument is that the adiabatic EPI (which accounts for how nuclear displacements alter the energies of the electron eigenstates and vice versa) should be of negligible thermodynamic importance because the EPI accounts for little change in the electron energy levels.[9] (This argument is probably more relevant for the nonadiabatic EPI, which is understood as a phonon coupling of unperturbed electron states across the Fermi surface.) Nevertheless, the importance of the EPI for the high-temperature thermodynamics of metals remains controversial. Quantitative calculations for nearly-free electron metals have predicted a significant contribution to the free energy from the adiabatic component of the EPI at temperatures up to melting.[10] Recently we showed experimentally that the EPI does have a large effect on the high-temperature thermodynamics of superconducting V_3Si and V_3Ge (with a contribution to the heat capacity larger than that of electrons or thermal expansion), and related this effect to the presence of sharp features in the electron density of states (DOS) near the Fermi level.[11] Here we show that the same effect occurs in V solid solutions, suggesting that this effect could be general.

The behavior of phonon frequencies as temperature increases, raising the phonon occupation numbers, is one of the central questions of high-temperature thermodynamics.[9,12] At high temperature, the extra vibrational entropy associated with softer (lower energy) phonon modes favors the expansion of the lattice. In the standard quasiharmonic model (QH), the rate of softening of the average phonon energy $\langle E \rangle$ is related to the rate of change in volume V of the crystal as:

$$\Delta\langle E\rangle/\langle E\rangle = -\bar{\gamma}\Delta V/V, \quad (1)$$

where $\bar{\gamma}$ is an average Grüneisen parameter.[9] In most materials, $\bar{\gamma} > 0$, and phonons soften upon thermal expansion. Microscopically, this thermal expansion and the associated shifts and broadenings of phonon frequencies stem from the anharmonic components in interatomic potentials, which are responsible for the PPI (scattering between harmonic phonon quasiparticles). Vanadium and the V-based dilute alloys investigated in this study all have similar (positive) thermal expansions. This would suggest similar PPIs and similar temperature dependencies of phonon DOS curves. However, our neutron-scattering measurements reveal a rather different picture.

For the present investigation, we performed inelastic neutron-scattering measurements of the phonon densities of states (DOSs) at temperatures from 10 K to 1300 K for pure V and solid solutions of V with 6 to 7at% of Nb, Co, or Pt solutes. We show that V-7%Co and V-6%Pt solid solutions have a normal quasiharmonic softening behavior with increasing temperature, whereas V and the isoelectronic V-6%Nb have an anomalous phonon stiffening. We relate the anomalous temperature behavior to an adiabatic EPI effect, associated with the broadening of electron states by phonons at high temperature. We report first-principles electronic structure calculations for vanadium and the alloys. We show that the experimental trends in the temperature dependence of the phonons are related to the filling of the *d*-band and the position of the Fermi level with respect to a peak in the electron DOS of V. Both heating and band filling result in a stiffening of the phonon DOS, and we explain this similarity through a common EPI effect originating with a peak in the electron DOS just below the Fermi level. The addition of *d* electrons to the system, through alloying with Co or Pt, suppresses the DOS at the Fermi level. Likewise, thermal broadening of the sharp peak in the electron DOS of pure V from

the Fermi-Dirac occupancy factor plus an adiabatic thermal broadening of the electron energy levels also suppresses the DOS at the Fermi level, removing a source of phonon softening.

II. EXPERIMENT

A. Synthesis

Alloys of V-7%Co, V-6.25%Nb, and V-6.25%Pt were prepared by arc-melting V slugs of 99.8% purity and pieces of Co, Nb, and Pt of 99.9% or better purity under a high-purity argon atmosphere. The mass loss upon arc melting was negligible and no oxidation was detected on the ingots. The samples were cold-rolled to the desired thicknesses, annealed in vacuum at 950 °C for an hour and quenched into iced brine. X-ray diffraction (XRD) measurements were performed on annealed powders with a Philips X'Pert series diffractometer using a Cu $K\alpha$ x-ray source. X-ray diffraction patterns for all samples were consistent with bcc solid solutions. Room temperature density measurements were conducted by a standard buoyancy technique.

B. Thermomechanical properties

Thermal expansion properties of V and V-7%Co were measured between 300 K and 900 K using a Perkin-Elmer TMA-7 thermomechanical analyzer with He purge gas to suppress oxidation. The measurement used cubic samples about 10 mm in length, cut from annealed ingots of V and V-7%Co with a low-speed diamond saw.

The heat capacity at constant pressure, C_P, was measured for pure V and V-7%Co, using a Netzsch DSC-404c differential scanning calorimeter. The measurements were conducted with Pt crucibles, Al_2O_3 liners, a heating rate of 20 K/min, and an ultrapure argon gas flow. In both the V and V-7%Co measurements, the reference sample was a synthetic sapphire disk, of mass comparable to the sample. Before every sample measurement, the instrument baseline with empty crucibles was measured, followed by a measurement of the reference sapphire in its crucible against an empty reference crucible. Additional differential measurements were performed by loading the sample and reference pans with V or V-Co samples and conducting differential measurements. The two samples were then switched and the two measurements averaged, to cancel out intrinsic differences between the two crucible thermocouples. Also, the number of atoms in both samples was matched to within a few percent, to have a similar thermal load in both pans. This procedure allows to accurately measure the difference in heat capacity between pure V and V-7%Co. Minimal oxidation was detected on the samples after runs up to 1673 K.

The bulk modulus, B, and the shear modulus, G, of the four materials were measured at room temperature with an ultrasonic pulse-echo setup. Several samples were cut from annealed ingots with a low-speed diamond saw, with sample thicknesses between 2 mm and 5 mm (the thickness and the face parallelism of each sample were measured with a precision micrometer).

C. Neutron scattering

Inelastic neutron scattering (INS) spectra were measured on the alloys V-6.25%Nb, V-6.25%Pt, and pure V using the Pharos time-of-flight chopper spectrometer at the Los Alamos Neutron Science Center. The samples were mounted in an AS Scientific ILL furnace, which was kept under high vacuum during all measurements. No oxidation was detected on the samples after the measurements. For measurements at low temperatures, the samples were encased in a thin-walled Al pan, and mounted into a Cu frame cooled by a closed-cycle He refrigerator. The incident neutron energy was $E_i = 75$ meV, and the energy resolution was about 0.8 meV at 40 meV neutron energy loss, increasing to about 3.0 meV at the elastic line. Additional measurements (pure V, 10 K to 775 K, and V-6%Nb, 10 K and 300 K) were acquired on the LRMECS chopper spectrometer at IPNS (Argonne National Laboratory) with similar experimental conditions.[13] The LRMECS measurements at high T were performed with a custom, low-background furnace.

All spectra were normalized by the total incident flux and sample mass and were corrected for detector efficiency and time-independent background. In all cases, the spectrum from the empty sample container was subtracted, and the elastic peak was removed. A standard procedure was used to correct for the effect of multiphonon scattering.[14] This analysis uses the incoherent-scattering approximation, which should be well satisfied for solid solutions of vanadium when solutes that scatter coherently are distributed randomly.

For pure elements of cubic crystals, this analysis provides the phonon DOSs. For an alloy, however, the phonon DOS obtained this way is "neutron-weighted." Because different isotopes have different efficiencies for scattering neutrons through phonon creation or annihilation processes, the modes corresponding to the elements of higher efficiency are overemphasized over those of elements with lesser neutron-scattering efficiency, resulting in a generalized phonon DOS. The ratios of neutron cross section over mass, σ/M, which determine the contribution of each species to the phonon DOS, are listed in Table I. It shows that Co solutes cause essentially no neutron weighting compared to V. The effect is also small for Nb and Pt solutes.

Inelastic neutron scattering spectra on V and V-7%Co were also measured on the HB2 three-axis spectrometer at the HFIR research reactor at Oak Ridge National Laboratory, using a constant $Q = 4.6$ Å^{-1}, a final energy of 14.8 meV, energy transfers from 50 to 2 meV, and an energy resolution of approximately 1 meV. The analysis procedures for the three-axis data were described previously.[16]

III. PHONON DENSITY OF STATES

The phonon DOS curves are shown in Fig. 1. The measurements on pure V with the Pharos and LRMECS time-of-flight neutron spectrometers are in very good agreement at all temperatures, and also with the three-axis data reported previously.[16] The anomalous lack of softening of the phonons in pure V is clearly seen in all measurements. The phonon DOS of V is essentially constant from 10 K to 1273 K, subject only to broadening. In the three-axis measure-

TABLE I. Samples and physical properties.

Sample	e/atom	$a_{300\ \mathrm{K}}$ (Å)	M_i (amu)	$\sigma_i^{\mathrm{scat}}/M_i$ [a] (barn/amu)	$G_{300\ \mathrm{K}}$ (GPa)	$B_{300\ \mathrm{K}}$ (GPa)	$\langle E\rangle_{300\ \mathrm{K}}$ [b] (meV)
Pure V	5.00	3.032 ± 0.002	50.94	0.100	48.1 ± 0.5	163 ± 4	23.0 ± 0.3
V-7%Co	5.28	3.006 ± 0.002	58.93	0.096	54 ± 1	171 ± 5	25.2 ± 0.2
V-6.25%Nb	5.00	3.051 ± 0.001	92.91	0.067	47.1 ± 0.5	165 ± 4	22.4 ± 0.2
V-6.25%Pt	5.31	3.034 ± 0.003	195.08	0.060	61.7 ± 0.5	176 ± 4	24.6 ± 0.2

[a]For minority species, using neutron cross sections from Ref. 15.
[b]From neutron-weighted phonon DOSs.

ments, it was found that this behavior changes at higher temperatures, and the phonon DOS of V softens between 1273 K and 1673 K.[16] The anomalous behavior from 10 K to 1273 K is particularly strong for the high-energy longitudinal modes between 26 meV and 31 meV, whose energy clearly increases with temperature. On the other hand, the low-energy transverse phonons soften between 10 K and 1273 K, but this softening is smaller than expected from thermal expansion over such a wide temperature range (see discussion below on expected quasiharmonic behavior).

The phonon DOS curves of V-6%Pt and V-7%Co behave more conventionally, softening gradually between 300 K and 1300 K. This softening apparently occurs for all the phonon modes in both alloys. The solutes Co and Pt also have comparable effects on the phonon DOS of V at room temperature, both causing a large stiffening of the vibrations, as previously reported.[13] On the other hand, isoelectronic Nb solutes only have a small effect on the phonon DOS and its dependence on temperature. The rather small effect of the heavy Nb solutes (about two times heavier than the host V atoms) indicates that the effect of mass difference is not very important for 6% Nb solutes. In the case of Pt solutes (about four times heavier than V), a resonance mode occurs around 12 meV,[17] but the effect of 6% Pt solutes on the phonon DOS is overall very similar to that of 7% Co solutes, whose mass is similar to that of V atoms. This indicates that electronic and bonding effects dominate over mass effects, and this is compatible with the similar numbers of d electrons/atom in the V-6%Pt and V-7%Co alloys,[13] given as the electron/atom ratio in Table I.

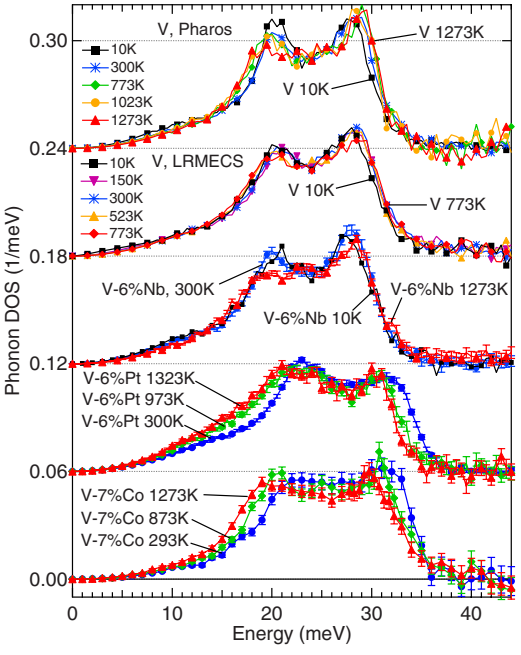

FIG. 1. (Color online) Phonon DOS of V alloys measured with inelastic neutron spectrometry.

The DOSs measured for the alloys are neutron-weighted. For the small solute concentrations considered here, however, the bias compared to the true phonon DOS would be small even if the neutron weights were significant. This was explicitly shown for the case of V-6%Pt, in which the partial phonon DOS for Pt atoms is substantially different from the phonon DOS of the host vanadium lattice.[17] Besides, it is expected that the neutron weighting should be only mildly temperature dependent, thus having minimal effects on the temperature trends discussed here.

The results from measurements of bulk and shear moduli are reported in Table I. The addition of a few percent of Co or Pt solutes in V strongly increases the elastic constants. The increase is larger for the shear modulus G ($\Delta G/G = 28\%$ and 12% for Pt and Co, respectively) than for the bulk modulus B ($\Delta B/B = 8\%$ and 5% for Pt and Co, respectively), but both are affected. On the other hand, Nb solutes have little effect on either G or B. The elastic constants are related to the stiffness of the dispersions for long-wavelength acoustic phonons. Table I offers a quick comparison with the mean phonon energies at 300 K, $\langle E\rangle_{300\ \mathrm{K}}$, obtained from the phonon DOSs. We note that the increase in $\langle E\rangle_{300\ \mathrm{K}}$ for 7%Co solutes is larger than for 6.25%Pt, although the elastic constants are less affected. Besides the difference in composition of the two alloys, this is likely due to the occurrence of a resonance mode for heavy Pt atoms (Ref. 17), which decreases the mean phonon energy $\langle E\rangle_{300\ \mathrm{K}}$, but should not affect the long-wavelength phonons and elastic constants as much.

IV. ANHARMONIC ENTROPY

The phonon entropy $S_{\mathrm{ph}}(V,T)$ is obtained from the phonon DOS $g_{V,T}(E)$ as:[9]

$$S_{\mathrm{ph}} = 3k_B \int \mathrm{d}E g_{V,T}[(n+1)\ln(n+1) - n\ln n], \qquad (2)$$

where $n=\{\exp[E/(k_{\mathrm{B}}T)]-1\}^{-1}$. The phonon entropy S_{ph} can be separated into a harmonic component, $S_{\mathrm{ph,H}}$, a component

representing the effect of dilation, $S_{ph,D}$, and a purely anharmonic component associated with the temperature dependence of the vibrations at a constant volume, $S_{ph,A}$:

$$S_{ph} = S_{ph,H} + S_{ph,D} + S_{ph,A}. \quad (3)$$

An important result of phonon thermodynamics is that Eq. (2) is still valid for the case of anharmonic vibrations, and that the full phonon entropy is obtained by using the experimental high-temperature phonon DOS measured by INS.[9]

The effect of lattice dilation on the total entropy, S_D, can be obtained from

$$S_D(T) = S_{el,D} + S_{ph,D} = 9\int_0^T Bv\alpha^2 dT', \quad (4)$$

where B is the isothermal bulk modulus, α is the linear coefficient of thermal expansion, and v is the specific volume (all dependent on temperature).[9] Although S_D represents the effect of dilation on both the electron and phonon entropies, ($S_{el,D}$ and $S_{ph,D}$, respectively), the first term is usually much smaller than the second. The sum of the harmonic and dilation components is usually called the quasiharmonic phonon entropy,

$$S_{ph,QH} = S_{ph,H} + S_{ph,D}, \quad (5)$$

and with this notation,

$$S_{ph} = S_{ph,QH} + S_{ph,A}. \quad (6)$$

In the harmonic limit, the phonon DOS does not change with temperature, so $S_{ph}(V,T)$ depends on temperature only through $n(T)$. Thus, it can be obtained from Eq. (2) using a DOS measured at a low temperature T_0: $S_{ph,H}(T) = S_{ph}^{g_{T_0}}(T)$ (typically, $T_0 = 10$ K or 300 K). We then obtain the nonharmonic portion of the phonon entropy, $S_{ph,NH}$, from the experimental phonon DOS:

$$S_{ph,NH} \equiv S_{ph} - S_{ph,H} = S_{ph,D} + S_{ph,A}. \quad (7)$$

We can thus compare the expected effect of thermal dilation, S_D, obtained from thermal expansion measurements, to values of $S_{ph} - S_{ph,H}$ derived from the neutron-scattering measurements of the phonon DOS at high temperature, and deduce the intrinsically anharmonic contribution, $S_{ph,A}$.

Results of the thermal expansion measurements for V and V-7%Co are shown in Fig. 2. The curve $S_D(T)$ was evaluated using Eq. (4) and is compared with $S_{ph} - S_{ph,H}$ obtained from neutron-scattering measurements in Fig. 3. For V-7%Co, thermal expansion accounts well for the nonharmonic behavior, $S_{ph,NH} \simeq S_D$. The agreement improves by adding the small electronic term, $S_{el,D}$, calculated from first principles (see below). For pure V, however, there is a large discrepancy between $S_{ph,NH}$ and S_D. To 1273 K, the anharmonic $S_{ph,A}$ for pure V is very similar in magnitude to $S_{ph,D}$, but of opposite sign, resulting in a zero (or very small) $S_{ph,NH}$.

The thermodynamic average Grüneisen parameter is defined by[19]

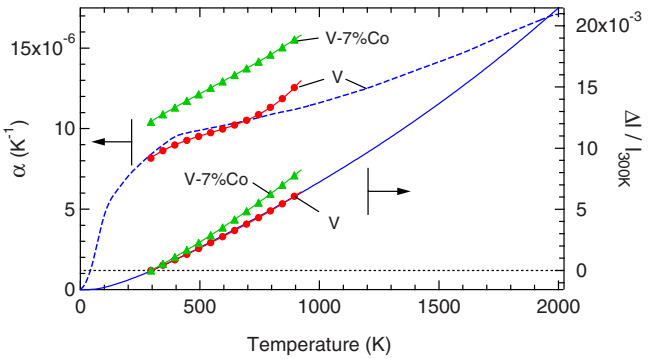

FIG. 2. (Color online) Linear thermal expansion and coefficient of linear thermal expansion for pure V and V-7%Co measured by dilatometry (markers) and literature values of Ref. 18 for pure V (lines). The differential expansion, $\Delta l/l$, is referenced to 300 K.

$$\bar{\gamma} = \frac{3\alpha V B_T}{C_V} = \frac{3\alpha V B_S}{C_P}, \quad (8)$$

where α is the linear coefficient of thermal expansion, B_T is (resp. B_S) the isothermal (resp. isentropic) bulk modulus and C_V is (resp. C_P) the heat capacity at constant volume (resp. pressure). Values of $\bar{\gamma}$ for V and V-7%Co were evaluated at 300 K from the measurements of the present work. We find that C_P is nearly equal for V and V-7%Co near 300 K. We find $\bar{\gamma}(\mathrm{V}) = 1.23$, and $\bar{\gamma}(\mathrm{V-7\%Co}) = 1.61$ (owing to a larger bulk modulus and a larger thermal expansion coefficient). The QH softening of the average phonon energy from thermal expansion was calculated from $\bar{\gamma}$ and α using Eq. (1) for pure V and V-7%Co. The Grüneisen parameter is known to vary little with temperature above room temperature.[19]

Figure 4 compares these QH results with the average phonon energies at different temperatures derived from the experimental phonon DOS curves. The average phonon frequency $\langle E \rangle$ for V-7%Co closely follows the QH behavior. This is in agreement with the results for the entropy shown in Fig. 3. On the other hand, there is a strong discrepancy between $\langle E \rangle$ from the high-T phonon DOS and the QH behavior for pure V. The phonon energies in V effectively stiffen

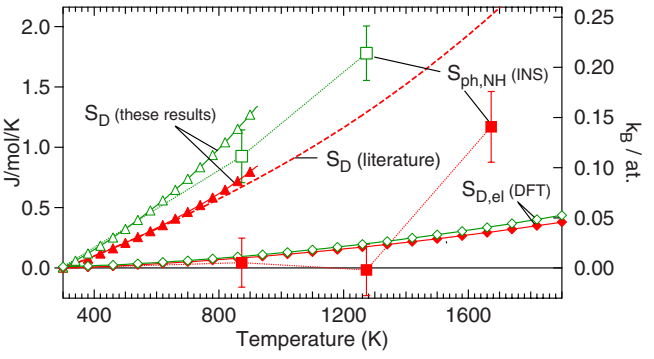

FIG. 3. (Color online) Anharmonic entropy for pure V and V-7%Co. The squares are the nonharmonic entropy $S_{ph,NH}$ calculated from INS data (HFIR); triangles are the entropy S_D calculated as in the text. Filled symbols: pure V, open symbols: V-7%Co. Dashed line: same as filled triangles, evaluated from the literature.

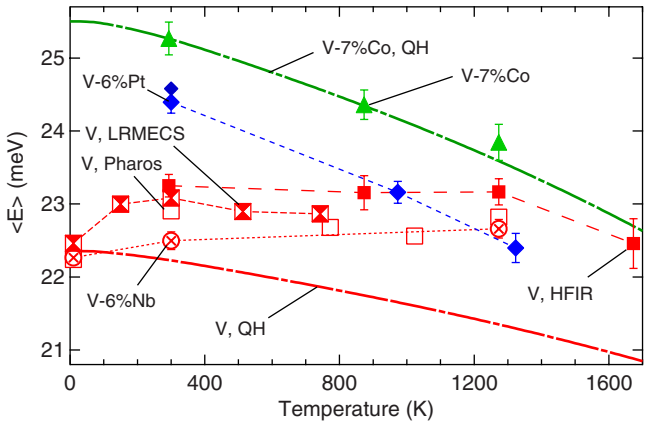

FIG. 4. (Color online) Mean phonon energy of V and alloys. The markers are results from INS measurements. The dashed-dotted lines correspond to QH behavior for V-7%Co and pure V, with experimental Grüneisen parameters (see text).

with increasing temperature, compensating for the effect of thermal expansion. We show in the following that this effect can be understood in terms of a coupling between the phonons and the electron band structure – an adiabatic electron-phonon interaction.

V. HEAT CAPACITY

Results for C_P of pure V and V-7%Co are shown in Fig. 5. Figure 5(a) shows the different components for the heat capacity of vanadium, and the curve recommended by Maglic for the total heat capacity of V, based on an assessment of several measurements reported in the literature.[20] Our differential scanning calorimetry (DSC) result for the total heat capacity of V (an average over five DSC runs) is in very good agreement with this recommended curve. The harmonic phonon contribution, $C_{\mathrm{ph,H}}$, was calculated from the V phonon DOS measured at 300 K (Pharos). The contribution from bare electrons, $C_{\mathrm{el,bare}}$, was derived from our electron entropy calculation with WIEN2K (results obtained from the electron DOS calculated with VASP were identical). The electronic heat capacity with the effect of the EPI broadening, $C_{\mathrm{el,e-p}}$, was also calculated from the first-principles electron DOS, as described below. The quasiharmonic contribution from thermal expansion, C_{D}, was derived from the respective entropy in Fig. 3, as $C_{\mathrm{D}}=T\partial S_{\mathrm{D}}/\partial T$. One can see that the sum of contributions, $C_{\mathrm{tot,bare}}=C_{\mathrm{ph,H}}+C_{\mathrm{D}}+C_{\mathrm{el,e-p}}$, is in excellent agreement with the measured total C_P. The effect of thermal expansion on the electronic heat capacity was not added to C_{el}, since it is already taken into account in C_{D} [Eq. (4)].

Our results for C_P of V-7%Co are shown in Fig. 5(b). The electronic specific heat was derived from the electron DOS for V-6.25%Co calculated with WIEN2K. The contribution from harmonic phonons, $C_{\mathrm{ph,H}}$, was calculated from the experimental phonon DOS of V-7%Co at 300 K. The quasiharmonic heat capacity due to thermal expansion, C_{D}, was obtained from the corresponding entropy in Fig. 3. Because our thermal expansion measurement is limited to $T<925$ K, the heat capacity for thermal expansion was also estimated over a larger range from the literature result for pure V.[18] The ratio of thermal expansions for V-7%Co and V is almost a constant over the whole range of our measurement (1.27 ± 0.01). Assuming a constant ratio, we obtained $\alpha(\mathrm{V-7\%Co})$ at higher temperatures by rescaling the literature result for $\alpha(\mathrm{V})$, and then calculated C_{D} for V-7%Co. For V-7%Co, $C_{\mathrm{tot,bare}}=C_{\mathrm{ph,H}}+C_{\mathrm{D}}+C_{\mathrm{el,e-p}}$ closely matches the measured total C_P. The curve labeled ΔC_P in Fig. 5(b) is the measured differential heat capacity of matched samples of V and V-7%Co $[C_P(\mathrm{V-7\%Co})-C_P(\mathrm{V})]$, showing that V-7%Co has a slightly higher heat capacity.

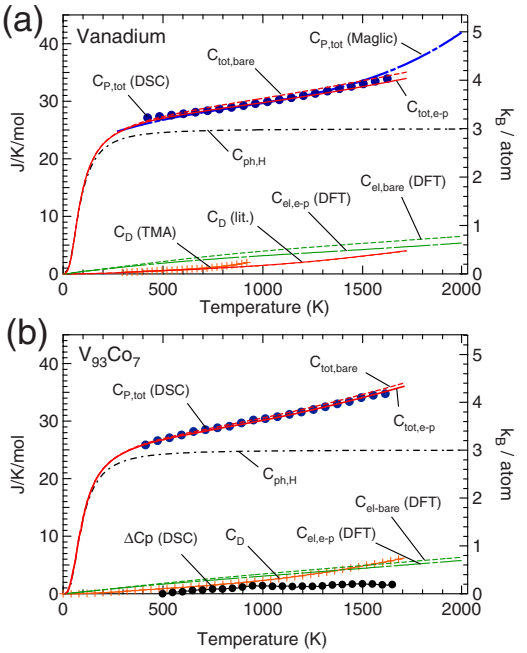

FIG. 5. (Color online) (a) Heat capacity of pure V and its different components. (b) Heat capacity of V-7%Co and its different components (see text). In both panels, the total constant pressure heat capacity, $C_{\mathrm{P,tot}}$, measured with DSC is given by the dots. Experimental error bars are comparable to the size of the markers. The sum of components are labeled $C_{\mathrm{tot,bare}}=C_{\mathrm{ph,H}}+C_{\mathrm{D}}+C_{\mathrm{el,bare}}$, and $C_{\mathrm{tot,e-p}}=C_{\mathrm{ph,H}}+C_{\mathrm{D}}+C_{\mathrm{el,e-p}}$. In panel *b*, $\Delta C_P=C_P(\mathrm{V-7\%Co})-C_P(\mathrm{V})$, measured with DSC. The value of C_P for pure V recommended by Maglic (Ref. 20) is shown in panel *a*.

VI. FIRST-PRINCIPLES CALCULATIONS

A. Methods

We performed density functional theory (DFT) computations of the electron density of states for bcc V and a series of V-6.25%X alloys, with X a transition metal solute. The disordered alloys were modeled as ordered $2\times2\times2$ supercells based on the B2 cubic unit cell, with the central V atom replaced by a solute atom X (for a concentration of 1 in 16, matching the experimental composition V-6.25%X). The calculations were performed with both WIEN2K (full-potential, linearized augmented plane waves)[21] and VASP (projector augmented waves).[22,23] The WIEN2K simulations used the Perdew-Burke-Ernzerhof generalized gradient approximation (GGA),[24] while VASP calculations were conducted with the

Perdew-Wang GGA.[25] The $2\times2\times2$ supercell calculations were conducted with a $10\times10\times10$ Monkhorst-Pack[26] **k**-point grid in WIEN2K and a $16\times16\times16$ grid in VASP, corresponding to 35 and 120 **k**-points in the irreducible portion of the Brillouin zone, respectively. The WIEN2K calculations were performed with $R_{\mathrm{MT}}\times k_{\mathrm{max}}=7.0$, while VASP calculations used the "accurate" setting for the kinetic energy cutoff. In the case of the magnetic Co solutes, spin-polarized calculations were performed on the relaxed $2\times2\times2$ supercells, and no magnetization on the solute atom was found. Subsequent calculations were performed with the non-spin-polarized model.

The total energy was minimized with respect to the supercell volume and the atom positions. The relaxation results from WIEN2K and VASP were in excellent agreement and the calculated change in lattice parameter upon alloying was within the experimental error bars of our measurements, although the absolute lattice parameter was consistently underestimated by about 1%.[27] Geometry optimizations were also conducted on $3\times3\times3$ supercells with composition $V_{53}X_1$, and these indicated that most of the relaxation occurs in the 1 NN shell around X. The changes in 1NN bond length calculated on the $2\times2\times2$ and $3\times3\times3$ supercells were in good agreement, indicating that effects are localized around each solute.[27]

Electron densities of states (DOSs) were obtained with WIEN2K using tetrahedron integration with 104 k-points and a Gaussian broadening of 3 mRy. DOS curves with a finer resolution were calculated with VASP, from the self-consistent electronic density obtained with the settings above, using a fine $30\times30\times30$ Monkhorst-Pack grid of k-points, and an energy resolution of 5 meV with the tetrahedron integration scheme.

B. Results

Results for the electron DOSs obtained with WIEN2K are shown in Fig. 6. The electron DOSs calculated with VASP were in excellent agreement with those obtained with WIEN2K. The electron DOSs for alloys of V with 6.25% of Ti, Cr, Mn, and Fe were also calculated.[27] For solutes close to V in the periodic table, we found a rigid-band behavior corresponding to the filling of the d band by the introduction of the extra d electrons from the solutes, increasing the Fermi energy (except for Ti solutes, which cause a depletion and a decrease in Fermi energy).[27] For late transition metal solutes such as Co or Pt, the distortions of the electron DOSs are more severe. This is expected since these solutes represent larger electronic disturbances and scatter electrons more strongly. However, some of the sharp peaks in the DOS for the alloys are probably caused by the artificially ordered structures used to model the dilute solid solutions. Some details of the calculated electron DOS would be washed away in disordered alloys, although the large peak associated with d states of Pt atoms (around −4.5 eV) is expected to remain. Both Co and Pt solutes have similar effects on the electron DOS around the Fermi level, resulting in similar shifts of the DOS to lower energies, yielding lower values of $N(E_{\mathrm{F}})$, and by approximately the same magnitude. On the other hand,

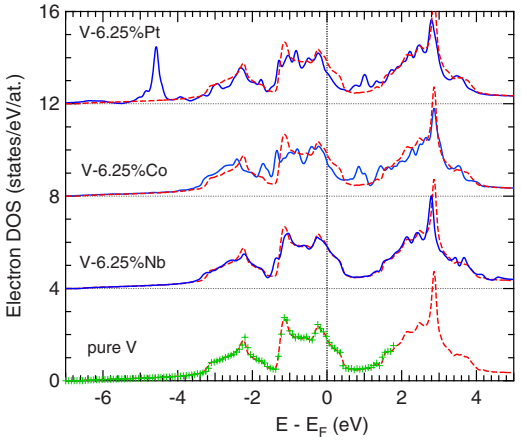

FIG. 6. (Color online) Electronic density of states for V-6.25%X alloys, computed from first principles with the DFT computer code WIEN2K (see text). The electron DOS for V is the dashed red line (repeated and offset for comparison) and the DOS for the V-6.25%X alloys are given by the solid blue lines. (Green crosses: electron DOS for V computed with VASP.)

isoelectronic Nb solutes induce very little change of the DOS.

The electron entropy at finite temperature is associated with the availability of unoccupied states above the Fermi level and is given by

$$S_{\mathrm{el}}=-k_{\mathrm{B}}\int_{-\infty}^{\infty}\mathrm{d}EN(E)\times[(1-f_{T,E})\ln(1-f_{T,E})+f_{T,E}\ln(f_{T,E})], \tag{9}$$

where $f_{T,E}$ is the Fermi distribution function and $N(E)$ is the electron density of states at energy E.[9] We computed the electronic entropy, S_{el}, of V and V-6.25%Co, using the electron DOS of Fig. 6. Using DFT, $N_V(E)$ can be calculated for different volumes V of the crystal, and the change in S_{el} with thermal expansion can be evaluated. A simple procedure is to calculate S_{el} at a low-temperature volume, V_{low}, and a high-temperature volume, V_{high}, and interpolate at intermediate temperatures:

$$S_{\mathrm{el}}(T)=S_{\mathrm{el}}(T,V_{\mathrm{low}})\left(\frac{T_{\mathrm{high}}-T}{T_{\mathrm{high}}-T_{\mathrm{low}}}\right)+S_{\mathrm{el}}(T,V_{\mathrm{high}})\left(\frac{T-T_{\mathrm{low}}}{T_{\mathrm{high}}-T_{\mathrm{low}}}\right). \tag{10}$$

We calculated the electron DOS at a low volume, corresponding to the optimized volume for WIEN2K calculations, and at a larger volume, corresponding to the dilation observed experimentally between 0 K and 900 K. The temperature-dependent entropy, $S_{\mathrm{el}}(T)$, was then obtained from Eq. (10). Results are plotted in Fig. 7. This figure also shows the part of the electron entropy associated with dilation, as calculated with Eq. (10). The effect of dilation on the electronic structure introduces only a small contribution on the scale of the total entropy of the system (about 1%). We note that $S_{\mathrm{el,D}}$ is positive, since a volume expansion leads to a reduction in electronic band width (smaller orbital over-

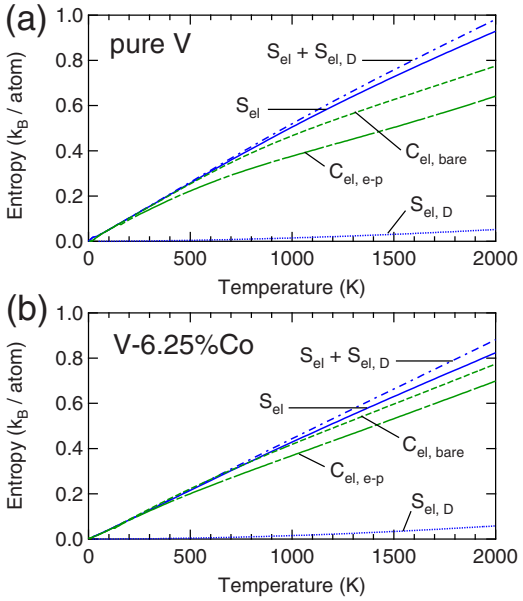

FIG. 7. (Color online) (a) Electronic entropy and heat capacity for pure V obtained from the electron DOS calculated from first principles. (b) Electron entropy and heat capacity for V-6.25%Co obtained from the electron DOS calculated from first principles.

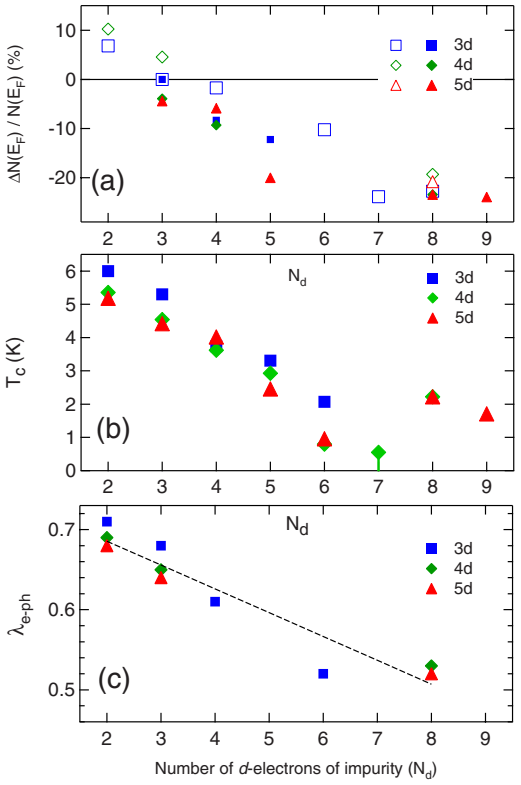

FIG. 8. (Color online) (a) Change in $N(E_F)$ for 6.25% TM solutes, from DFT calculations (open markers) and heat capacity in the literature (solid markers). (b) Estimated superconducting critical temperature for solid solutions V-6.25%TM, as function of the number N_d of d electrons of the TM solute (in the $3d$, $4d$ or $5d$-series). (c) Calculated λ_{el-ph} from T_c measurements in literature (see text). The number of d electrons of V is taken equal to 3.

lap), and consequently an increase in height of the DOS.

The electronic heat capacity, $C_{el,bare}$, was obtained from S_{el}, as $C_{el,bare}=TdS_{el}/dT$. Results are shown in Fig. 7. Also shown in this figure is the electronic heat capacity with the effect of EPI broadening of energy levels, $C_{el,e-p}$, discussed below.

Because of the negative slope of $N(E)$ at the Fermi level, the introduction of solutes raises (decreases) $N(E_F)$ when the solutes have fewer (more) d electrons than vanadium. Experimental values of $N(E_F)$ were linearly interpolated from values of the low-temperature electronic specific heat reported in the literature for V-X alloys with 5% to 10% solutes. Details are given in Ref. 27. The change in the density of states at the Fermi level calculated from first principles is also plotted in Fig. 8(a), as a function of the number of d electrons of the solutes (N_d). A large decrease in $N(E_F)$ occurs by alloying with late transition metals (TM), owing to the steep negative slope of the electron DOS of pure V around E_F. The calculated values are in good agreement with values of $N(E_F)$ derived from low-temperature heat capacity measurements, also plotted in Fig. 8(a).

VII. SUPERCONDUCTING PROPERTIES

Elemental vanadium is a superconductor with a transition temperature $T_c=5.3$ K, one of the highest for pure elements.[12] This suggests a fairly strong electron-phonon coupling, as quantified by the parameter λ, related to the electronic density at the Fermi level and the average phonon energy. In the McMillan theory of strong-coupled superconductors,[28] the electron-phonon coupling constant λ is

$$\lambda = \frac{N(E_F)\langle I^2\rangle}{M\langle\omega^2\rangle}, \tag{11}$$

where $N(E_F)$ is the electron density at the Fermi level E_F, $\langle I^2\rangle$ is the average over the Fermi surface of the square of the electron-phonon interaction matrix element, M is the nuclear mass, and the average phonon frequency square $\langle\omega^2\rangle$ is

$$\langle\omega^2\rangle = \frac{\int d\omega\omega\alpha^2(\omega)g(\omega)}{\int d\omega\alpha^2(\omega)g(\omega)/\omega}, \tag{12}$$

where $\alpha^2(\omega)g(\omega)$ is the direction-averaged Éliashberg coupling function. (From prior work on V and Nb, $\alpha^2(\omega)g(\omega)$ is very similar to the phonon DOS $g(\omega)$, and one can use the experimental $g(\omega)$ to estimate $\langle\omega^2\rangle$.[29,30]) The superconducting transition temperature in McMillan's theory, revised by Allen and Dynes,[13] is

$$T_c = \frac{\langle\hbar\omega\rangle_{\log}}{1.20\times k_B}\exp\left[\frac{-1.04(1+\lambda)}{\lambda-\mu^*(1+0.62\lambda)}\right], \tag{13}$$

where μ^* is the effective Coulomb repulsion potential for the electrons and $\langle\hbar\omega\rangle_{\log}$ is the logarithmic average of the phonon energy.[31]

Using published measurements of T_c for V-X alloys with solute concentrations less than 10% (typically 5% and 10% solutes), we linearly extrapolated the value of T_c for alloys of V-6.25%X. Our results are shown in Fig. 8(b). We calculated λ for the V-6.25%X alloys with Eq. (13), using our measurements of average phonon energies, and setting $\mu^*=0.13$ for the effective Coulomb repulsion, a value commonly used for transition metals. Results are shown in Fig. 8(c). A significant suppression in λ occurs for later TM solutes, with an approximately linear decrease with the number of *d* electrons of the solute, N_d. This decrease in λ is expected from the decrease in $N(E_F)$ and the stiffening of phonons [cf. Eq. (11)]. What is important from Fig. 8 is the correlation between band filling and λ. Although not all of the states at the Fermi level are expected to contribute equally to the EPI, with band filling there is a monotonic decrease in λ, a trend reported by others.[1]

VIII. ADIABATIC BROADENING OF ELECTRON STATES

In pure V, the effectiveness of the electron-phonon coupling decreases with increasing temperature, because of both the change in electronic occupation functions at finite temperature, and the thermal broadening of electron levels.[12,32] To assess the latter, we performed an analysis of the electron DOS with the approach of Ref. 33. In this analysis, the electron levels have a finite lifetime and energy width at $T>0$ K, owing to the distortions of the lattice induced by the phonons. The resulting electronic broadening function is a Lorentzian function, $\mathcal{L}_\Gamma$, of full-width-at-half-maximum (FWHM) $2\Gamma=2\pi\lambda k_B T$.[12,33] The broadened electron DOS, $\tilde{N}(E)$, is obtained by convolution, $\tilde{N}(E)=\mathcal{L}_\Gamma(E)*N(E)$. The shift in electron chemical potential $\mu(T)$ was calculated consistently, by integrating $\tilde{N}(E)\times f_{T,\mu}(E)$ and equating it to the total number of electrons in the system. Results for $N(E)$ and $\tilde{N}(E)$ are shown in Fig. 9(b) for pure V ($\lambda=0.7$) and $V_{15}Co_1$ ($\lambda=0.5$). Numerical results for the integral number of states around μ are given in Table II.

The thermal broadening of the electron DOS results in a monotonic decrease in $N(E_F)$ in pure V to temperatures of 1000 K or higher. We find $\tilde{N}(\mu(T=1000\text{K}))/\tilde{N}(\mu(T=0\text{K}))=-23\%$, but $\tilde{N}(\mu)$ is less affected in the case of $V_{15}Co_1$ (−13%). For pure V, high temperatures suppress the ability of the conduction electrons to screen the nuclear motions, resulting in stiffer phonons. As pointed out in Ref. 32, the EPI broadening of the electron levels should be self-limiting, since it tends to decrease λ at higher temperature, so a more accurate self-consistent result should lie between the unbroadened and broadened DOS in Fig. 9.

The broadening of the electron DOS by the EPI has a direct effect on the electron entropy and heat capacity. We calculated the electronic heat capacity for the broadened DOS at different temperatures, $C_{el,e-p}(T)$. Results are shown in Fig. 7. The decrease in $N(E_F)$ induced by the EPI broadening causes a significant suppression in C_{el}, particularly in the case of pure V. Our results for pure V are in qualitative agreement with those of Thiessen,[33] although we do not find any crossing of $C_{el,bare}$ and $C_{el,e-p}$.

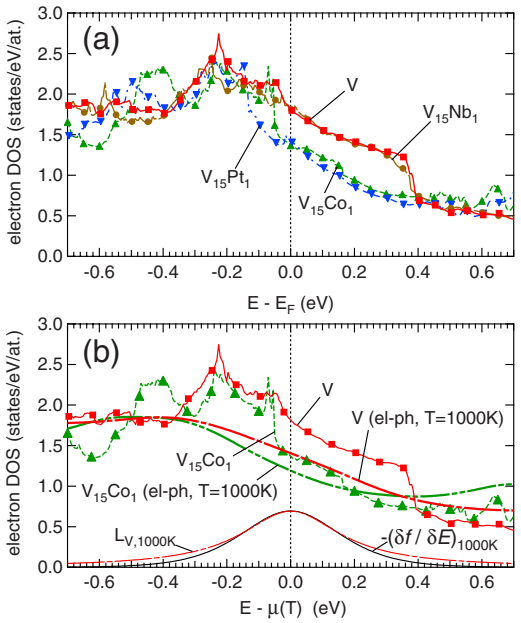

FIG. 9. (Color online) (a) Electronic DOS for V and $V_{15}X_1$ computed from first principles with VASP. (b) Electronic DOS for V and $V_{15}Co_1$ at 0 K and with broadening effect induced by the EPI at 1000 K and shift in $\mu(T)$ ($\lambda(V)=0.7$, $\Gamma(V)=190$ meV; $\lambda(V-6.25\%Co)=0.5$, $\Gamma(V-6.25\%Co)=135$ meV. Also shown are the derivatives of the Fermi-Dirac function $-\frac{\partial f}{\partial E}(E,T=1000\text{ K})$ and the Lorentzian representing the EPI broadening for V at 1000 K ($\Gamma=190$ meV).

Besides a decrease in the number of states at E_F, the shape of the Fermi surface changes significantly upon band filling, changing the spanning vectors responsible for the nonadiabatic EPI. A topological electronic transition occurs around 5.4 electrons/atom, corresponding to the disappearance of the octahedral hole pocket around Γ, and a necking of the jungle-gym tubes from Γ to H. This can be seen as a discontinuity in $N(E)$ at $E-E_F=0.37$ for V and $V_{15}Nb_1$ and at $E-E_F=0.15$ in $V_{15}Co_1$ [Fig. 9(a)]. However, it is expected that details of the Fermi surface should affect mostly the nonadiabatic EPI at low temperatures. For the adiabatic EPI at higher temperatures, the fine features of the Fermi surface will be washed away by thermal disorder in the periodicity of the lattice.

TABLE II. Electronic densities at Fermi level (VASP) and integrated densities within Fermi-Dirac broadening window [see Fig. 9(b)] around chemical potential $\mu(T)$ for pure V and V-6.25%Co. The electron DOS broadened by the EPI is denoted as $\tilde{N}(E)$.

	$N(E_F)$	$\langle N(E)\rangle$	$\langle\tilde{N}(E)\rangle$ [a]
	$T=0$ K (e/eV/at.)	$T=1000$ K (e/at.)	$T=1000$ K (e/at.)
V	1.82	0.52	0.40 ($\lambda=0.7$)
$V_{15}Co_1$	1.37	0.43	0.35 ($\lambda=0.5$)
$(V_{15}Co_1\text{-}V)/V$	−25%	−17%	−13%

[a]Electron DOS broadened by EPI, included as Lorentzian broadening of width $2\Gamma=2\pi\lambda k_B T$ (FWHM).

IX. DISCUSSION

A. Elastic moduli and phonons

Elastic moduli, especially shear moduli, are known to be sensitive to the electronic structure of bcc transition metals and alloys.[34–37] Anomalous temperature dependencies have been reported for elastic constants of bcc Nb- and V-based alloys, in particular for the shear constant C_{44}.[38–41] For pure V, C_{44} softens normally below about 500 K, then stiffens from 500 K to about 1600 K, and finally reverts to a normal softening above 1600 K to melting.[41] A very similar behavior was found in pure Nb.[39] It is known that the nonadiabatic EPI should couple only weakly to transverse phonon modes, owing to the zero contribution of modes with transverse polarization in the electron-phonon scattering matrix element, except in "umklapp" processes.[12,42] This rules out the nonadiabatic EPI as an explanation for the anomalous behavior in C_{44}. Our measurements of the V phonon DOS (Fig. 1) show that the transverse phonon modes soften a little between 10 K and 773 K in pure V, but much less so than in V-7%Co and V-6%Pt. The nonadiabatic EPI is expected to affect longitudinal phonons at cryogenic temperature, however. This is confirmed by our measurements, which show that the longitudinal modes of vanadium stiffen from 10 K to 300 K (Fig. 1). This stiffening at low temperature is also seen in the mean phonon energy (Fig. 4). The increase in $\langle E\rangle$ with T below 300 K appears particularly strong. It could be associated with a stronger temperature dependence of the nonadiabatic EPI, compared to the adiabatic EPI, but this may also be an effect of lower thermal expansion at low temperature. The broadening of electron states by the adiabatic EPI is small at low T.

At higher temperature ($T>300$ K), the adiabatic component of the EPI is expected to dominate,[10] and both the shear elastic constant and the phonon DOS are affected by the thermal broadening of electron states. The adiabatic EPI stiffening in this temperature range compensates for the softening from thermal expansion, leading to (anomalously) constant phonon DOS, $\langle E\rangle$, and C_{44}. We note that both the smearing of occupation numbers by the Fermi-Dirac statistics and the broadening of electron levels by phonons (adiabatic EPI) should contribute to the phonon stiffening at intermediate temperatures, as both decrease the number of occupied electron states around the Fermi level. First-principles electronic structure calculations identified the effect of band filling on the bulk modulus and shear moduli in V and Nb alloys, in agreement with experimental alloying trends.[34–40] However, previous interpretations considered only the smearing of electron occupation numbers by the Fermi-Dirac distribution at high temperature. The calculations based on this effect do not reproduce the temperature range over which the effects are measured for C_{44} of bcc niobium.[34] Our results show that the additional smearing of electronic features by phonons at high temperature (broadening the electron states themselves, rather than just their occupations) are important to understand the temperature dependence of phonons and elastic constants in these materials. The adiabatic EPI induces a significant additional smearing, in some sense increasing the effective temperature. It is expected that by including the additional EPI-induced broadening of the electron states, the range of temperature over which the elastic constants behave anomalously could be better matched by first-principles simulations. This was pointed out early on by Bujard *et al.*, who performed measurements and calculations of elastic constants in bcc Nb-Mo alloys.[39] The adiabatic EPI mechanism (combined with Fermi-Dirac smearing) should saturate by the highest temperatures, when the peak in the electron DOS around E_F is fully smeared out. This is in good agreement with our phonon measurements in pure V above 1300 K (see Fig. 4 and Ref. 16), and also in agreement with the high-temperature shear modulus measurements reported in the literature.[39,41]

Figure 4 shows that the softening of the average phonon energy $\langle E\rangle$ for V-7%Co is in excellent agreement with the effect of thermal expansion predicted by the quasiharmonic model, $\Delta\langle E\rangle/\langle E\rangle=-\bar{\gamma}\Delta V/V$. The V-6%Pt alloy follows a similar trend, although its $\langle E\rangle$ is suppressed at all temperatures by resonance modes of massive Pt atoms.[17] (An alloy of V-31%Cr, which has a similar electron-to-atom ratio to that of V-7%Co, also showed a similar behavior from 10 K to 300 K.) On the other hand, Fig. 4 shows that $\langle E\rangle$ for pure V and V-7%Nb deviate substantially from the thermal behavior predicted by the quasiharmonic model. The adiabatic EPI effect is thus strongly dependent on alloying, which can be understood as a dependence on the position of the Fermi level with respect to the peak in the electron DOS.

The phonon frequencies of Fig. 4 show a clear correlation to the electron DOS of Fig. 9, consistent with a common EPI for both chemical and thermal effects. Adding 7%Co to V suppresses the EPI and causes an increase in $\langle E\rangle$ by 2 meV at room temperature. The effect of temperature over a range of 1000 K is similar, being about 1.5 meV (compare the offset of the INS data to the QH curve in Fig. 4). The decrease in electron DOS at E_F caused by adding 6.25%Co is approximately comparable to the effect of temperature at 1000 K (Fig. 9). The calculated effect of temperature on $N(E)$ in Fig. 9 is likely an overestimate, however, as the EPI-induced broadening should be self-limiting. The EPI broadening effect at 1000 K should be a bit weaker than that of adding 0.3d-electrons/atom, in accord with the experimental results. We also point out that the expected decrease in λ with temperature [related to the decrease in $N(E_F)$, Eq. (11)] may play a role in the negative curvature of the electrical resistivity of V at elevated temperatures.[43]

B. Heat capacity

Our calorimetry measurements show that V-7%Co has a slightly larger heat capacity than pure V (by about $0.2k_B$/atom between 1000 K and 1500 K, see Fig. 5), despite its smaller electronic heat capacity (lower $N(E)$ around E_F, see Fig. 9). The larger total heat capacity in V-7%Co can be related to the greater softening of its phonons.[44] In pure V, the sum of contributions to the heat capacity from harmonic phonons, lattice dilation (elastic energy of expansion), and bare electrons [$C_{\mathrm{tot,bare}}$ in Fig. 5(a)] is slightly larger than the total heat capacity. The suppression in C_{el} from the EPI-induced broadening of the electron DOS brings the sum of

components ($C_{\mathrm{tot,e-p}}$ in Fig. 5) in excellent agreement with the measured total heat capacity, especially in the range of 700 K–1300 K. At $T>1500$ K, the V heat capacity rises above $C_{\mathrm{tot,e-p}}$, possibly because the phonons start softening. In V-7%Co, the EPI-induced suppression in C_P is smaller, and both $C_{\mathrm{tot,bare}}$ and $C_{\mathrm{tot,e-p}}$ are in good agreement with the measured total C_P [Fig. 5(b)].

It appears that the adiabatic EPI is responsible for the suppression of C_P in pure V, compared to the higher C_P of V-7%Co, for which phonons soften normally. This is in agreement with the calculations of Allen and Hui, who predicted an effect of the adiabatic EPI on the high-temperature heat capacity of metals.[44] Allen and Hui also predicted a doubling of this contribution, owing to mirror contributions in the heat capacities of phonons and electrons, both being corrected by a term $-C_{\mathrm{ph,H}} \times d\langle \ln \omega \rangle / d \ln T$ (with $\hbar\omega$ the temperature-dependent phonon energy levels).[44] However, we note that in V, the EPI reduces the electronic heat capacity ($C_{\mathrm{el,e-p}} - C_{\mathrm{el,bare}}$ in Fig. 7), but the lack of softening of phonons does not seem to yield a doubling of this contribution (as evidenced by the agreement of $C_{\mathrm{tot,e-p}}$ and $C_{\mathrm{P,tot}}$ in Fig. 5). It is possible that the fortuitous cancellation of the EPI-induced stiffening by the tendency of phonons to soften upon lattice dilation causes a cancellation of this extra contribution in the case of pure V ($\langle \hbar\omega \rangle$ is almost constant from 300 K to 1300 K in V). Another possibility is that part of the suppression in C_P is already accounted for by a smaller dilation component, C_{D}. As can be seen in Fig. 2, pure V expands less than V-7%Co (despite a smaller bulk modulus in V than in V-7%Co). This can also be understood from the EPI effect, since the impeded phonon softening in pure V prevents the gain in vibrational entropy that ought to compensate for the elastic energy cost of lattice expansion. In V-7%Co, the phonons soften normally upon increasing T (and V), as the EPI-induced stiffening is weaker, and thermal expansion is not impeded. Pure V is still expected to expand, as a lack of expansion would cause an even larger EPI-induced stiffening of phonons and an unfavorable loss of vibrational entropy.

C. Adiabatic electron-phonon interaction and features in the electron density of states

We suggest that the same effect occurs for phonons in Nb,[7,8] which exhibit an anomalous stiffening with temperature, because the band structure of Nb is essentially the same as for V. A very similar alloying trend has been reported for the temperature dependence of C_{44} in V-Cr and Nb-Mo alloys.[39,40] The effects observed in the dilute V-based alloys are very similar to those we recently reported for ordered A15 V_3X compounds up to 1273 K (Ref. 11) (and also reported by others at cryogenic temperatures[45]). Many materials with sharp peaks in their electron DOSs close to the Fermi level have phonons with temperature dependencies that depart from quasiharmonic behavior. Although neutron-scattering measurements have established that phonons in Pd and Pt soften with increasing temperature,[46] Eriksson *et al.* report negative anharmonic phonon entropies $S_{\mathrm{ph,A}}$ for both Pd and Pt, indicating that these materials soften less than expected based on the quasiharmonic model.[47] Calculations of the electron DOSs of fcc Pd and Pt by Eriksson *et al.* and others show a sharp peak at the Fermi level, at the upper edge of the d band.[47] Nickel has a similar electron DOS, but is more complex because of magnetism. Although Eriksson *et al.* did not elaborate further, the negative $S_{\mathrm{ph,A}}$ of Pd and Pt, their electron DOSs, and the fact that these elements have significant electron-phonon coupling constants ($\lambda \sim 0.4$, and 0.6 for Pd and Pt, respectively[1]) indicates that the same effect could be occurring in these materials as in bcc V and Nb. This is corroborated by measurements of elastic constants as function of temperature in Pd, which revealed an anomalous stiffening of the C_{44} shear modulus.[48,49] The anomaly in C_{44} in Pd is suppressed upon alloying with Rh or Ag,[49] as expected from the discussion above.

On the other hand, the opposite effect may occur in metals whose Fermi level lies in a narrow valley or at the bottom of a peak in the electron DOS. In such a case, the broadening of the DOS by the adiabatic EPI should raise the electron density at the Fermi level, tending to soften the phonons. The Fermi level in bcc Cr, Mo and W lies in the upper part of the pseudo-gap,[47] and thus it is possible that the large phonon softening observed in Cr and Mo,[50,51] and the large positive values of $S_{\mathrm{ph,A}}$ for Cr, Mo and W,[47] may originate with the adiabatic EPI effect. Aluminum metal has a relatively flat and featureless electron DOS and shows little deviation from quasiharmonic behavior.[52]

Phonon anharmonicity from the adiabatic EPI mechanism originates from thermal broadening of the sharp features of the electron DOS at the Fermi level, corresponding to a broadening of electronic states near the Fermi surface. In the adiabatic approximation, this broadening originates with the effects of thermal atomic displacements induced by phonons at elevated temperature. Such an adiabatic effect is well-suited for calculation with density functional theory in the Born-Oppenheimer approximation. Preliminary DFT calculations of the effect of static lattice distortions (representing snapshots of thermal disorder) on the electron DOS of A15 V_3Si revealed a qualitative agreement with the broadened electron DOS obtained with the same convolution procedure described above. More detailed calculations are necessary, however, to treat the EPI effect self-consistently for phonons and electrons. Nevertheless, DFT simulations in the Born-Oppenheimer approximation seem capable of predicting the effect of the adiabatic EPI on high-temperature thermodynamics.

X. CONCLUSION

Inelastic neutron scattering was used to measure the phonon DOS of pure bcc V and alloys of V with Co, Nb, and Pt solutes at elevated temperatures. Normal quasiharmonic softening of the phonons was observed for V-7at%Co and V-6at%Pt, but there was little change with temperature of the phonon DOSs of pure V and V-6at%Nb. Some differences in heat capacity and thermal expansion were also observed between pure V and V-7at%Co. These differences are explained by differences in the adiabatic EPI, which tends to smear out sharp features in the electron DOS.

Thermodynamically-significant effects of the EPI exist to two-thirds of the melting temperature of V—a surprising result considering common assumptions about, and many calculations of, the effect of the EPI on the free energy of metals.[12] However, such a possibility was suggested by early theoretical papers considering EPI effects on the heat capacity and spin susceptibility,[44,53] and by recent calculations of the free energy of simple metals.[10]

In the case of V solid solutions, alloying and temperature cause similar changes in the electron DOS near the Fermi level and similar effects on the phonons of V. For pure V, the Fermi level is on a peak of the electronic DOS, allowing many electrons to be affected by thermal disorder. With increasing temperature, the thermal broadening of the electron energy levels washes out the peak in the electron DOS, decreasing the electronic density at the Fermi level, and suppressing the ability of the electrons to screen forces on ions. This effect should be general, and is discussed in light of a number of results in the literature. We suggest that studies of phonons at high temperatures may provide useful information on the EPI. More generally, we expect that a thermodynamic description reliant on independent phonons and electron excitations may be inadequate for materials whose electron DOS has sharp features near the Fermi level.

ACKNOWLEDGMENTS

We thank F. Trouw, M. Hehlen, J. L. Robertson, and E. Goremychkin for help with neutron-scattering experiments. We thank J. McCorquodale for help with computing systems. This work has benefited from the use of LANSCE at the Los Alamos National Laboratory and IPNS at the Argonne National Laboratory, funded by the U.S. DOE under Contracts No. W-7405-ENG-36 and DE-AC02-06CH11357. Use of Oak Ridge National Laboratory was also supported by the U.S. DOE. This work was supported by DOE BES Grant No. DE-FG02-03ER46055.

[1] P. B. Allen, in *Handbook of Superconductivity*, edited by C. P. Poole, Jr. (Academic, New York, 1999), Chap. 9, p. 478.
[2] Y. Ding, R. Ahuja, J. Shu, P. Chow, W. Luo, and H. K. Mao, Phys. Rev. Lett. **98**, 085502 (2007).
[3] W. Luo, R. Ahuja, Y. Ding, and H. K. Mao, Proc. Natl. Acad. Sci. U.S.A. **104**, 16428 (2007).
[4] M. Ishizuka, M. Iketani, and S. Endo, Phys. Rev. B **61**, R3823 (2000).
[5] A. Landa, L. Klepeis, P. Söderlind, I. Naumov, O. Velikokhatnyi, L. Vitos, and A. Ruban, J. Phys.: Condens. Matter **18**, 5079 (2006).
[6] B. M. Powell, P. Martel, and A. D. B. Woods, Phys. Rev. **171**, 727 (1968); Can. J. Phys. **55**, 1602 (1977).
[7] S. M. Shapiro, G. Shirane, and J. D. Axe, Phys. Rev. B **12**, 4899 (1975).
[8] F. Güthoff, B. Hennion, C. Herzig, W. Petry, H. R. Schober, and J. Trampenau, J. Phys.: Condens. Matter **6**, 6211 (1994).
[9] D. C. Wallace, *Statistical Physics of Crystals and Liquids* (World Scientific, Singapore, 2002).
[10] N. Bock, D. Coffey, and D. C. Wallace, Phys. Rev. B **72**, 155120 (2005); N. Bock, D. C. Wallace, and D. Coffey, *ibid.* **73**, 075114 (2006).
[11] O. Delaire, M. S. Lucas, M. Kresch, and B. Fultz (unpublished).
[12] G. Grimvall, *The Electron-Phonon Interaction in Metals* (North-Holland, Amsterdam, 1981).
[13] O. Delaire and B. Fultz, Phys. Rev. Lett. **97**, 245701 (2006).
[14] M. Kresch, O. Delaire, R. Stevens, J. Y. Y. Lin, and B. Fultz, Phys. Rev. B **75**, 104301 (2007).
[15] V. F. Sears, Neutron News **3**, 26 (1992).
[16] P. D. Bogdanoff, B. Fultz, J. L. Robertson, and L. Crow, Phys. Rev. B **65**, 014303 (2001).
[17] O. Delaire, T. Swan-Wood, and B. Fultz, Phys. Rev. Lett. **93**, 185704 (2004).
[18] Y. S. Touloukian, R. K. Kirby, R. E. Taylor, and P. D. Desai, *Thermophysical Properties of Matter* (IFI/Plenum, New York, 1975), Vol. 12.
[19] G. Grimvall, *Thermophysical Properties of Materials* (North-Holland, Amsterdam, 1999).
[20] K. D. Maglić, Int. J. Thermophys. **24**, 489 (2003).
[21] P. Blaha, K. Schwarz, and P. Sorantin, Comput. Phys. Commun. **59**, 399 (1990).
[22] G. Kresse and J. Furthmüller, Comput. Mater. Sci. **6**, 15 (1996).
[23] G. Kresse and D. Joubert, Phys. Rev. B **59**, 1758 (1999).
[24] J. P. Perdew, K. Burke, and M. Ernzerhof, Phys. Rev. Lett. **77**, 3865 (1996).
[25] J. P. Perdew, K. Burke, and Y. Wang, Phys. Rev. B **54**, 16533 (1996).
[26] H. J. Monkhorst and J. D. Pack, Phys. Rev. B **13**, 5188 (1976).
[27] O. Delaire, Ph.D. thesis, California Institute of Technology, 2006; http://etd.caltech.edu/etd/available/etd-05262006-160244
[28] W. L. McMillan, Phys. Rev. **167**, 331 (1968).
[29] S. Y. Savrasov and D. Y. Savrasov, Phys. Rev. B **54**, 16487 (1996).
[30] B. N. Harmon and S. K. Sinha, Phys. Rev. B **16**, 3919 (1977).
[31] P. B. Allen and R. C. Dynes, Phys. Rev. B **12**, 905 (1975).
[32] K. M. Ho, M. L. Cohen, and W. E. Pickett, Phys. Rev. Lett. **41**, 815 (1978).
[33] M. Thiessen, Int. J. Thermophys. **7**, 1183 (1986).
[34] L. Huang, L. Vitos, S. K. Kwon, B. Johansson, and R. Ahuja, Phys. Rev. B **73**, 104203 (2006).
[35] Y. Ohta and M. Shimizu, J. Phys. F: Met. Phys. **13**, 761 (1983).
[36] K. W. Katahara, M. H. Manghnani, and E. S. Fisher, J. Phys. F: Met. Phys. **9**, 773 (1979).
[37] J. T. Lenkkeri, J. Phys. F: Met. Phys. **10**, 611 (1980).
[38] J. Ashkenazi, M. Dacorogna, M. Peter, Y. Talmor, E. Walker, and S. Steinemann, Phys. Rev. B **18**, 4120 (1978).
[39] P. Bujard, R. Sanjines, E. Walker, J. Ashkenazi, and M. Peter, J. Phys. F: Met. Phys. **11**, 775 (1981).
[40] P. Bujard and E. Walker, Solid State Commun. **43**, 65 (1982).
[41] E. Walker, Solid State Commun. **28**, 587 (1978).
[42] J. M. Ziman, *Electrons and Phonons* (Clarendon, Oxford, 1960).
[43] P. D. Desai, H. M. James, and C. Y. Ho, J. Phys. Chem. Ref.

Data **13**, 1097 (1984).
[44] P. B. Allen and J. C. K. Hui, Z. Phys. B **37**, 33 (1980).
[45] B. P. Schweiss, B. Renker, E. Schneider, and W. Reichardt, in Proceedings of the Second Rochester Conference on Superconductivity in d- and f-Band Metals, 1976, edited by D. H. Douglass (Plenum, New York, 1976), p. 189.
[46] *Phonon States of Elements, Electron States and Fermi Surfaces of Alloys*, Landolt-Börnstein, New Series, Group III, Vol. 13, Pt. A, edited by K.-H. Hellwege and O. Madelun (Springer, Berlin, 1981), and references therein.
[47] O. Eriksson, J. M. Wills, and D. C. Wallace, Phys. Rev. B **46**, 5221 (1992).
[48] C. Weinmann and S. Steinemann, Phys. Lett. **47A**, 275 (1974).
[49] E. Walker, J. Ortelli, and M. Peter, Phys. Lett. **31A**, 240 (1970).
[50] J. Trampenau, W. Petry, and C. Herzig, Phys. Rev. B **47**, 3132 (1993).
[51] J. Zarestky, C. Stassis, B. N. Harmon, K.-M. Ho, and C. L. Fu, Phys. Rev. B **28**, 697 (1983).
[52] M. Kresch, M. Lucas, O. Delaire, J. Y. Y. Lin, and B. Fultz, Phys. Rev. B **77**, 024301 (2008).
[53] W. E. Pickett, Phys. Rev. Lett. **48**, 1548 (1982).